The amyloidogenicity of gelsolin is controlled by proteolysis and pH

Gayathri Ratnaswamy[1], Edward Koepf[1], Haimanot Bekele[1], Helen Yin[2] and Jeffery W Kelly[1]

Background: Normally, gelsolin functions in plasma as part of the actin-scavenging system to assemble and disassemble actin filaments. The Asp187→Asn (D187N) and Asp187→Tyr (D187Y) gelsolin mutations facilitate two proteolytic cuts in the parent protein generating a 71-residue fragment that forms amyloid fibrils in humans, putatively causing Finnish type familial amyloidosis (FAF). We investigated the role of the D187N mutation in amyloidogenicity using biophysical studies *in vitro*.

Results: Both the recombinant wild-type and D187N FAF-associated gelsolin fragments adopt an ensemble of largely unfolded structures that do not self-associate into amyloid at pH 7.5. Incubation of either fragment at low pHs (6.0–4.0) leads to the formation of well-defined fibrils within 72 hours, however.

Conclusions: The D187N mutation has been suggested to destabilize the structure of the gelsolin parent protein (specifically domain 2), facilitating two proteolytic cleavage events. Our studies demonstrate that generating the largely unstructured peptide is not sufficient alone for amyloid formation *in vitro* (on a time scale of months). A drop in pH or an analogous environmental change appears necessary to convert the unstructured fragment into amyloid fibrils, probably through an associative mechanism. The wild-type gelsolin fragment will make amyloid fibrils from pH 6 to 4 *in vitro*, but neither the wild-type fragment nor fibrils have been observed *in vivo*. It is possible that domain 2 of wild-type gelsolin is stable in the context of the whole protein and not susceptible to the proteolytic degradation that affords the 71-residue FAF-associated peptide.

Addresses: [1]Department of Chemistry and the Skaggs Institute for Chemical Biology, The Scripps Research Institute, 10550 North Torrey Pines Road, La Jolla, CA 92037, USA. [2]Department of Physiology, University of Texas Southwestern Medical School, 5323 Harry Hines Boulevard, Dallas, TX 75235, USA.

Correspondence: Jeffery W Kelly
E-mail: jkelly@scripps.edu

Key words: amyloid, gelsolin, pH dependent, proteolysis, recombinant

Received: **12 November 1998**
Revisions requested: **11 December 1998**
Revisions received: **21 January 1999**
Accepted: **5 February 1999**

Published: **19 April 1999**

Chemistry & Biology May 1999, **6**:293–304
http://biomednet.com/elecref/1074552100600293

© Elsevier Science Ltd ISSN 1074-5521

Introduction

Human gelsolin is expressed both as an 81 kDa intracellular protein and as a secreted 84 kDa extracellular polypeptide [1,2], each composed of six domains. Gelsolin functions in at least three ways: it binds two actin monomers to nucleate actin polymerization; it can bind to filamentous actin and sever the noncovalent bonds of the polymer; and it caps the rapidly polymerizing end of F-actin following severing. These functions are activated by micromolar Ca^{2+} concentrations and possibly by pHs < 6 [3]. Extracellular gelsolin is thought to be an important component of the actin-scavenging system that removes actin released from dead cells into the bloodstream [4]. An Asp187→Asn (D187N) or Asp187→Tyr (D187Y) mutation in domain 2 of the 84 kDa secreted form of gelsolin allows a single proteolytic event between Arg172 and Ala173 during secretion [5]. Upon arrival in the plasma, a secondary proteolytic event occurs, which results in a 71-residue gelsolin fragment (residues 173–243) that is sometimes found deposited in the cranial or peripheral nerves, the cornea and in a variety of other tissues in individuals with Finnish type familial amyloidosis (FAF) [5]. These deposits have the morphology and dye-binding properties characteristic of amyloid fibrils associated with a variety of neurodegenerative diseases [6–9].

Significant insight into the structure–function relationships of human gelsolin was revealed when the crystal structure of highly homologous horse plasma gelsolin was solved [10]. In terms of the structure of domain 2, proteolytic processing of domain 2 position 187 variants results in the removal of strands 1 and 3 (shown in gray in Figure 1), which probably alters the structure of the 71-residue 173–243 gelsolin FAF-associated fragment, owing to the deletion of one integral and one exterior β strand [10,11]. The crystal structure demonstrates that the position of the FAF-associated mutations (at residue 187) are proximal to the disulfide bond between the Cys188 and Cys201 residues linking strands 4 and 5, probably destabilizing the extracellular form of gelsolin directly by interfering with disulfide-bond formation or by interfering with the hydrogen bonding between the Asp187 sidechain and its partners (Asn184, Lys166 and Gln164; Figure 1), or both [10,11]. The apparent importance of the Asp187 sidechain for protein structure and/or

Figure 1

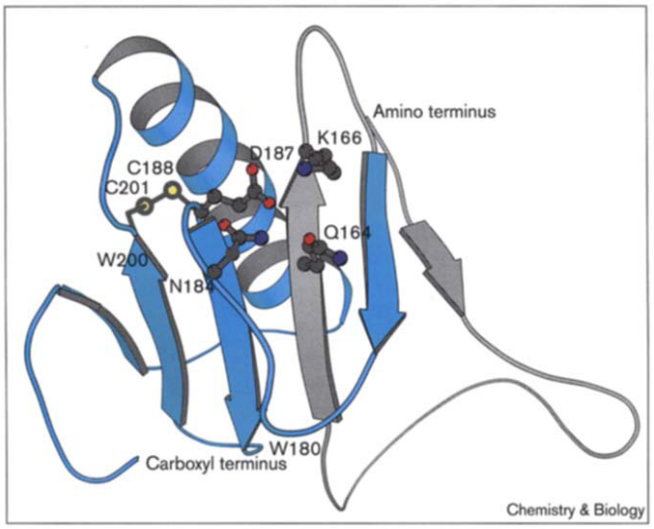

Ribbon diagram representation of the polypeptide backbone of the horse plasma gelsolin S2 domain. The other five domains have been omitted for clarity. The amyloidogenic fragment (173–243) is cyan, whereas the remainder of the S2 domain is gray. The sidechain of the FAF-associated mutation (Asp187) is illustrated along with the sidechains of Gln164, Lys166 and Asn184, residues that are within hydrogen bonding distance of Asp187. The disulfide bond between Cys188 and Cys201 and the location of the tryptophan residues (W) are also indicated. This figure was prepared using MOLSCRIPT [73].

function is reflected in the fact that this residue is highly conserved in the gelsolin family of proteins.

Studies with nine- and 11-residue peptides from gelsolin (residues 183–191 and 182–192, respectively) reveal that these small peptides that incorporate the FAF-associated mutation D187N or D187Y form amyloid-like fibrils, whereas the wild-type nonapeptide might not (the undecapeptide is weakly amyloidogenic via a Congo red assay but not by a thioflavine T-based fluorometric evaluation) [12]. These results imply that the mutations themselves directly control amyloid formation [12]. Peptide fragments of amyloidogenic proteins can give misleading results, however, as some peptides not associated with amyloid sequences can form amyloid-like fibrils *in vitro* [13,14] (H. Lashuel and J.W.K., unpublished observations). Here, we evaluate the amyloidogenicity and conformational stability of both the wild-type and D187N FAF-associated gelsolin fragments. The fragments studied have a Gly–Ser– (GS–) sequence attached to the amino terminus of the 71-residue amyloidogenic fragment as a result of the recombinant expression system employed. Somewhat surprisingly, the wild-type gelsolin fragment GS–173–243 is amyloidogenic (the opposite to what was observed by analysis of short peptides), albeit slightly less so than the D187N GS–173–243 gelsolin variant [12]. Interestingly, both the wild-type and D187N GS–173–243 gelsolin variants form amyloid fibrils within 72 h after encountering slightly acidic conditions *in vitro* — that is, proteolysis of the parent gelsolin protein does not appear to be sufficient for amyloid fibril formation within a 3 month observation period at pHs higher than 6.0, 37°C. Low pH conditions probably lead to protonation of key carboxylate and imidazole sidechains, in addition to probably altering the distribution of largely unordered conformational states, allowing assembly-mediated conformational changes and ultimately amyloid fibril formation to occur on a time scale that allows biophysical studies to be performed. It might be that conditions other than a low pH environment convert gelsolin very slowly into amyloid fibrils *in vivo* (on a time scale of years); we have yet to identify these conditions, however. The results of this study suggest that the predominant effect of the mutations is to enable proteolysis of the parent protein.

Results

Expression, purification and characterization of wild-type and D187N GS–173–243 fragments of gelsolin

The gelsolin 173–243 fragment was expressed as an amino-terminal His-tagged glutathione S-transferase (GST) fusion protein incorporating a thrombin cleavage site between $(His)_6$GST and the gelsolin 173–243 polypeptide [15]. Purification of the soluble fusion protein was achieved by passing the total cell lysate through glutathione sepharose affinity resin, eluting the fusion protein with 10 mM reduced glutathione at pH 8. Bovine thrombin was added directly to the fusion protein in the glutathione elution buffer to liberate the 71-residue gelsolin peptide. The wild-type and D187N gelsolin fragments contain two extra amino acids at their amino-terminal ends (GS–), an artefact of the recombinant expression system used to create the peptides. The GST protein was removed from the GS–173–243 gelsolin peptide by passing the reaction mixture through a Ni-NTA column. The Ni-NTA elutant containing gelsolin GS–173–243 was concentrated by ultrafiltration and purified to homogeneity using gel filtration chromatography. Electrospray ionization mass spectrometry (ESI–MS) confirmed that the masses of the wild-type GS–173–243 fragment (8136.8 amu) and the D187N GS–173–243 fragment (8135.6 amu) are correct. The mass spectrometric measurements were consistent with oxidized gelsolin GS 173–243 — that is, gelsolin having an intramolecular disulfide bond. This interpretation was confirmed by preparing disulfide oxidized and reduced forms of both wild-type and D187N GS–173–243 gelsolin. Reverse-phase high performance liquid chromatography (HPLC) analysis demonstrated that the recombinant GS–173–243 gelsolin used in these studies co-elutes with the oxidized standard of gelsolin GS–173–243, Figure 2. To evaluate the suitability of gelsolin for amyloidogenicity and biophysical studies, sedimentation equilibrium analytical

Figure 2

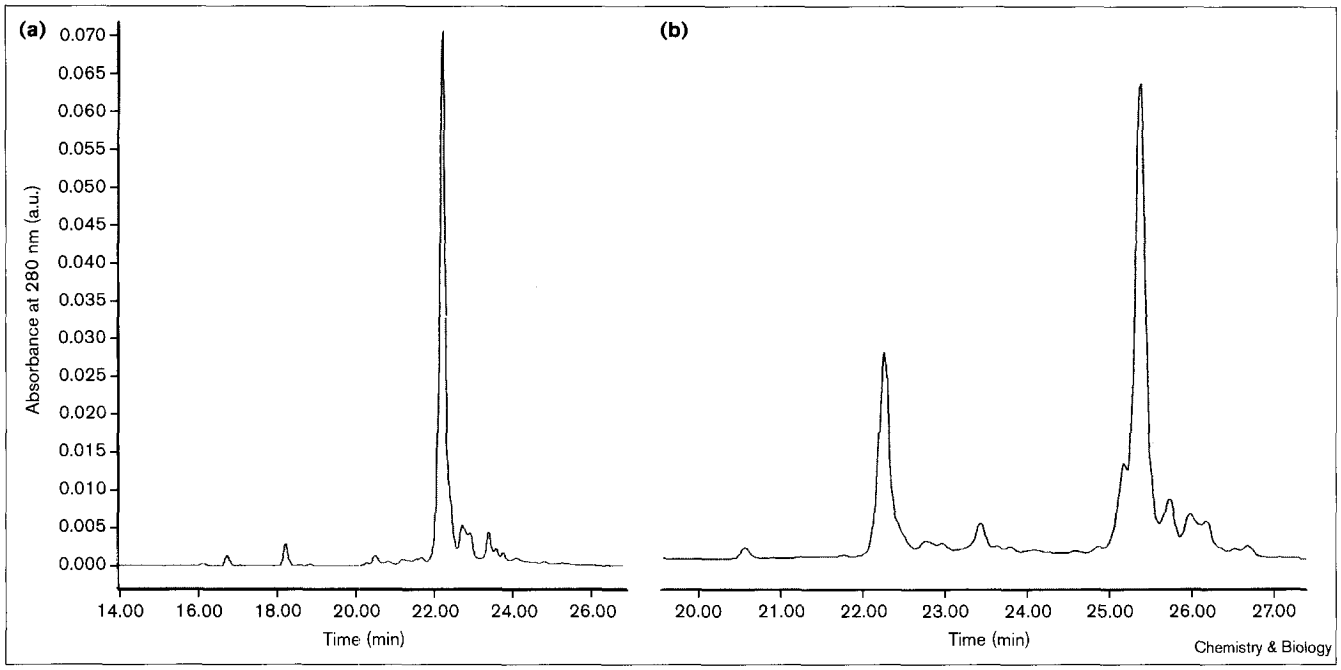

Reverse phase HPLC analysis of wild-type GS–173–243 gelsolin to probe the oxidation state of Cys188 and Cys201. **(a)** HPLC chromatogram of freshly purified recombinant wild-type gelsolin, which exhibits a retention time of 22.1 min (oxidized). **(b)** HPLC chromatogram of co-injected oxidized and reduced gelsolin exhibiting retention times of 22.1 and 25.4 min, respectively.

ultracentrifugation studies were performed on gelsolin to evaluate its quaternary structure, or lack thereof, in aqueous solution. The gelsolin concentration distribution as a function of radial distance along the cell fits to an ideal species model having a solution molecular weight of 8135 ± 148 Da, demonstrating the monomeric nature of wild-type and D187N gelsolin (25 μM) at pH 7.4 (see the Supplementary material section). Gelsolin GS–173–243 does not readily aggregate as a 25 μM solution at pH 7.4, making it feasible to study its conformational properties at neutral pH and amyloidogenicity under acidic conditions.

Evaluating the amyloidogenicity of wild-type and D187N GS–173–243 gelsolin

The amyloidogenicity of purified gelsolin (GS–173–243) at either 0.2 mg/ml (25 μM) or 0.02 mg/ml (2.5 μM) was evaluated as a function of pH using 0.5 pH unit steps over the range of 4.0–7.5 (100 mM NaCl). The samples were incubated at 4°C or 37°C for several days to several months and evaluated using light scattering and Congo red binding analysis (a dye that shows selectivity for amyloid fibrils) [16]. Samples that appeared not to exhibit amyloid fibril formation by the methods mentioned above were evaluated further using electron microscopy (EM) to probe whether the absence of fibrils was due to the inability to detect them by optical methods. Neither the wild-type 73-residue gelsolin peptide nor the FAF-associated D187N variant peptide form amyloid fibrils over the pH range of 7.5–6.0 after incubation for 72 h at 37°C. We have been unable to detect amyloid fibrils in 25 μM wild-type and D187N GS–173–243 gelsolin samples incubated at pH 7.5 for more than a month by light scattering and electron microscopy analysis. Interestingly, both the wild-type and, to a greater extent, the D187N FAF-associated GS–173–243 gelsolin fragments (25 μM) readily form amyloid fibrils over the pH range of 6.0 to 4.0 within 72 h (Figure 3). Gelsolin fibril formation is concentration dependent; no fibril formation was observed for either the wild-type or D187N gelsolin 73-residue fragments incubated at a concentration of 2.5 μM over 2 months (pH 7.5–4.0). An EM study of a 25 μM sample of wild-type (Figure 4a) and D187N (Figure 4b) GS–173–243 gelsolin incubated at pH 4 forms well-defined amyloid fibrils as visualized employing 1% uranyl acetate as a negative contrast agent. The Fourier-transform infrared (FT–IR) spectra of wild-type (Figure 5a) and D187N (Figure 5b) GS–173–243 gelsolin fibrils are virtually identical and exhibit the amide I stretch (amide C=O stretch) at 1623 cm^{-1} and a high frequency band at 1692 cm^{-1} characteristic of β-sheet structure in the amyloid core (Figure 5) [6,17]. The wild-type GS–173–243 amyloid fibrils do not exhibit the classical red-shifted Congo red spectrum exhibited by the D187N GS–173–243 gelsolin amyloid fibrils, however, suggesting that there might be subtle differences between wild-type and variant fibrils. Temperature also appears to be very important for gelsolin amyloid fibril formation. The mutant

Figure 3

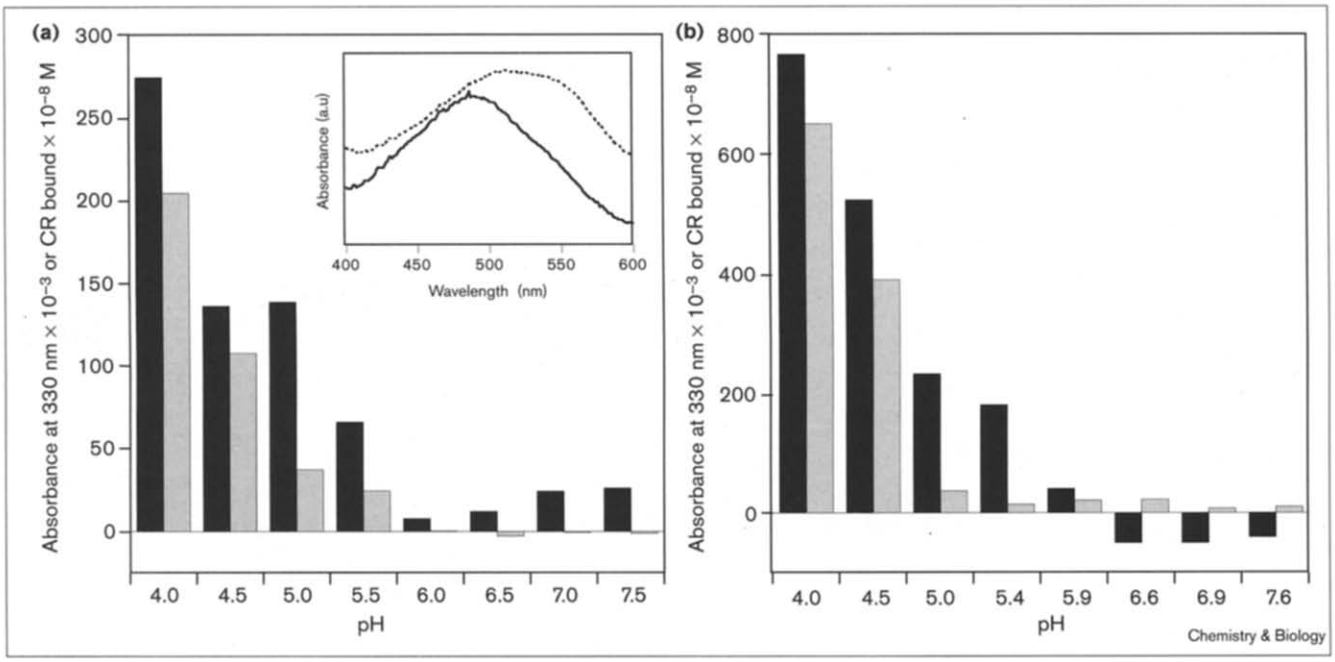

Evaluating gelsolin amyloidogenicity as a function of pH. **(a)** Light scattering (black bars) and Congo red (CR) binding (gray bars) analyses of wild-type GS–173–243 gelsolin amyloid fibril formation as a function of pH. The inset displays the visible spectra for the addition of 550 µl of a 10 µM Congo Red solution to a 100 µl suspension of wild-type (solid line) and D187N (dashed line) GS–173–243 gelsolin fibrils prepared as described in the Materials and methods section (gelsolin fibril formation assays). This comparison demonstrates the lack of a red shift in the binding of Congo red to wild-type gelsolin fibrils. **(b)** Bar graph representing an analogous study evaluating the amyloidogenicity of the D187N gelsolin variant. Gelsolin amyloidogenicity was studied employing 25 µM GS–173–243 samples (50 mM buffer, 100 mM NaCl) after incubation at 37°C for 72 h.

GS–173–243 fragment will only inefficiently form amyloid fibrils at 4°C — that is, only after 2 months of incubation (25 µM D187N gelsolin GS–173–243 at pH 4). The salt dependence associated with gelsolin (GS–173–243) fibril formation is also very interesting; 100 mM NaCl enables fibril formation, whereas 25 mM NaCl does not allow fibril formation to occur at otherwise optimal conditions. The rate of gelsolin fibril formation is much faster if the sample is inverted once every hour, implying that shearing of growing amyloid fibrils accelerates their growth, which might be attributed to seeding. Ongoing mechanistic experiments are needed to understand the rate acceleration associated with agitation.

Conformational analysis of the wild-type and D187N GS–173–243 gelsolin monomers

The key questions going into this study regarding the conformation of the gelsolin amyloidogenic fragment were, firstly, is there residual structure in the 173–243 fragment? and, secondly, are there pH or other environment-dependent conformational changes that explain the amyloidogenicity of wild-type and D187N gelsolin discussed above? The structure of the 73-residue gelsolin amyloid fragment was probed using a number of spectroscopic methods including far-UV circular dichroism (CD), ^{1}H nuclear magnetic resonance (NMR) including H/D exchange studies, tryptophan-fluorescence anisotropy measurements, and ANS-fluorescence-based binding studies. Neither the wild-type nor the D187N variant of gelsolin GS–173–243 exists as a structured polypeptide in solution under the conditions evaluated in this study. Both wild-type and D187N gelsolin GS–173–243 appear to adopt a family of largely unordered structures, in which the ensemble of states is only partially constrained by a disulfide bond and possibly other weak interactions.

In the structured environment of a folded protein, the rotational mobility of tryptophan residues is restricted. Tryptophan residues in a rigid environment exhibit a maximal anisotropy value of ~0.17 (excitation at 280 nm) [18]. The measured single-point tryptophan-fluorescence anisotropy values of ~0.06 derived from the Trp180 and Trp200 residues in both the wild-type and the D187N variant are pH independent (Figure 6) suggesting that there are no defined conformational changes detected in the local environment of the tryptophan residues that are mediated by changes in pH. The far-UV CD data that characterizes both the wild-type and D187N FAF-associated variant GS–173–243 gelsolin are consistent with a lack of regular secondary structure (there is an intense

Figure 4

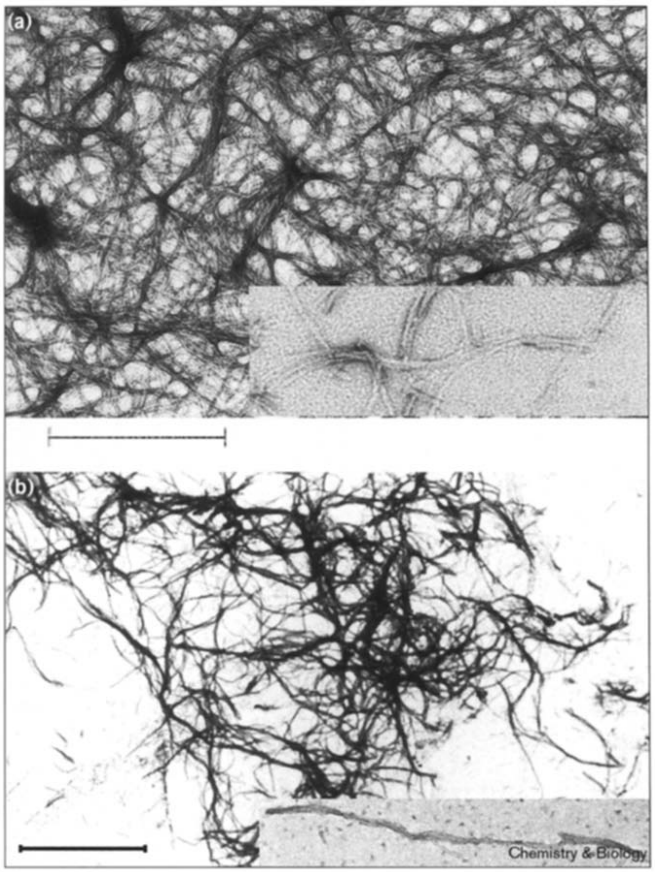

Transmission electron microscopy characterization of gelsolin fibrils. **(a)** Electron micrograph of wild-type gelsolin fibrils obtained by incubating the gelsolin peptide fragment at pH 4.0, 37°C (in 50 mM acetate, 100 mM NaCl). The average diameter of the wild-type fibrils is 180 ± 10 Å. Scale bar, 1μm. **(b)** Electron micrograph of the D187N gelsolin fragment obtained using the same conditions for the wild-type sample. The average diameter of the D187N fibrils is 230 ± 10 Å. Scale bar, 2 μm. The insets in both the figures are magnified views of a single fibril.

minimum centered around 197 nm at both pH 7 and pH 4 after less than 1 h incubation at 4°C; Figure 7). These data demonstrate that the unaggregated unordered structure formed at pH 4 under conditions ultimately capable of fibril formation is not distinguishable from the structure formed at pH 7; there are, therefore, no easily discernible pH-mediated conformational changes. The lack of dispersion in the upfield methyl region (no peaks upfield of 0.7 ppm), as well as in the downfield amide region (no peaks downfield of 8.6 ppm) of the ^{1}H NMR spectrum confirms the absence of well-defined secondary and tertiary structure (Figure 8). Dissolution of lyophilized gelsolin into deuterated buffer at pH 7.4 (not corrected for the D isotope effect) shows complete exchange of the gelsolin amide protons after 5 min, the dead time of the NMR manual mixing experiment (folded proteins exhibit protection against H/D exchange for most residues participating in intramolecular hydrogen bonding). Furthermore, the chemical shifts of the indole NH protons (Trp180 and Trp200) overlap at a chemical shift of 10.18 ppm, a value expected for a tryptophan residue in a random coil [19]. Lastly, the inability of GS–173–243 gelsolin to bind ANS at pH 7.4 and 4.4 relative to the significant binding characterizing the gelsolin A-state formed at pH 2 is consistent with a largely unordered structure lacking organized hydrophobic patches (Figure 9) [20–23].

Discussion

The results outlined above document that both the wild-type and D187N FAF-associated variant gelsolin fragments GS–173–243 can form amyloid fibrils *in vitro* over the pH range of 6.0–4.0 on a time scale commensurate with biophysical measurements. Interestingly, only D187N gelsolin is proteolytically cleaved into the 71-residue amyloidogenic fragment and transformed into amyloid fibrils *in vivo* [24–28]. Neither proteolysis nor fibril formation has ever been observed for wild-type gelsolin in humans. The probable reason for this is that the wild-type gelsolin protein (organized into six folded domains) does not get cleaved to make the 173–243 fragment, owing to its increased stability or folding rate relative to the D187N gelsolin protein [5,11,29–34]. The D187N mutation might destabilize this portion of the gelsolin protein or slow down its rate of folding making it susceptible to proteolysis. It seems likely that proteolysis would facilitate rapid unfolding of the liberated 173–243 fragment. The timing, degree of and rate of unfolding relative to the two proteolytic events is currently unknown, however, and is the subject of ongoing studies in our laboratory.

An important finding of this study is that proteolysis appears to be necessary, but not sufficient, for gelsolin amyloid fibril formation (GS–173–243). The simulation of physiological conditions (pH 7.5, 37°C, 100 mM NaCl) does not appear to be sufficient to convert either the wild-type or the D187N gelsolin amyloidogenic fragment into amyloid fibrils on a time scale allowing biophysical experiments (< 3 months). Dropping the pH below 6.0 facilitates amyloid fibril formation, however, allowing us to study the mechanism of gelsolin amyloidosis on a time scale of days. The pH dependence of gelsolin GS–173–243 fibril formation is interesting because a number of amyloid proteins, including Aβ, amylin, gelsolin and transthyretin form amyloid fibrils optimally under acidic conditions around pH 5 [35–43]. These observations suggest that amyloid fibril formation could occur in an acidic organelle such as an endosome or lysosome, or via the intermediacy of the acidic extracellular matrix, something we are investigating further employing cell biology approaches [44–49]. At the present time, however, we have no evidence for endosomal or lysosomal involvement in amyloid fibril formation in humans.

Figure 5

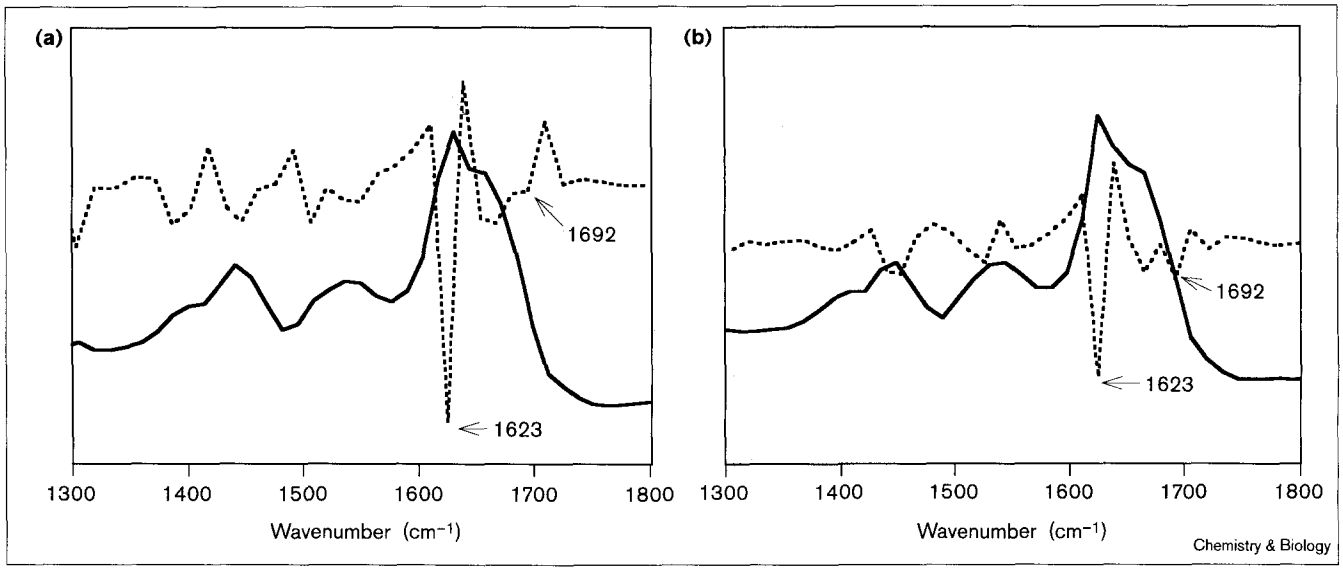

Infrared analysis of the secondary structure of gelsolin amyloid. **(a)** FT–IR spectra of fibrils formed from the wild-type gelsolin fragment. **(b)** FT–IR spectra of fibrils formed by the D187N variant. The solid lines represent the observed data and the dotted lines are the second derivative spectra. The amide I stretches are identified by arrows.

It is important to realize that environmental changes other than pH changes could also facilitate gelsolin fibril formation *in vivo*.

The D187N or D187Y mutation neutralizes the charge at position 187, which by itself is not sufficient to make the gelsolin GS–173–243 amyloidogenic (see the pH 7.5 data, Figure 3) on an experimental timescale. Changing the charge state on gelsolin by lowering the pH (protonating the carboxylate and imidazole sidechains) probably influences the ensemble of unordered conformations and probably favors aggregation, which appears to drive the β-sheet structural transition and the higher-order assembly thought to be important for amyloid fibril formation [50,51]. Lowering the pH does not appear to facilitate a detectable unstructured to structured transition in the monomer (Figure 7); it is reasonable, therefore, to propose that self-assembly mediates the observed structural changes observed in the fibril (Figure 5). The salt dependence associated with gelsolin (GS–173–243) fibril formation is also very interesting and probably manifests itself in the assembly reaction by screening unfavorable charge–charge interactions. It is not yet clear whether gelsolin amyloid fibril formation is susceptible to seeding [52]. Interestingly, the rate of gelsolin amyloid fibril formation is markedly increased by inverting the unseeded gelsolin solution once every hour. Further experiments are necessary to understand these interesting results.

Figure 6

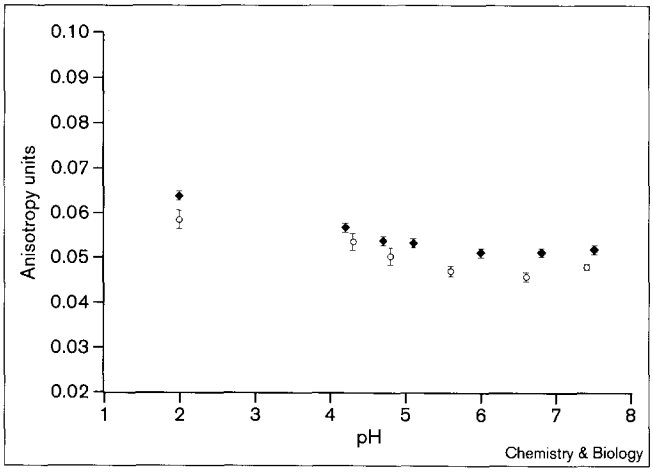

Tryptophan-fluorescence anisotropy measurements as a function of pH for the wild-type (◆) and the D187N (O) GS–173–243 gelsolin peptides. The measurements were made on 1 μM gelsolin samples at 20°C. Each point on the graph represents an average of 25 measurements.

Understanding the mechanism by which a soluble protein is transformed into a largely insoluble β-sheet rich quaternary structure, referred to as an amyloid fibril, is critical for further understanding the role that these fibrils or their precursors play in human disease [9,53,54]. The amyloid hypothesis invokes the process of amyloid fibril formation as the causative agent in human amyloid disease, a hypothesis

Figure 7

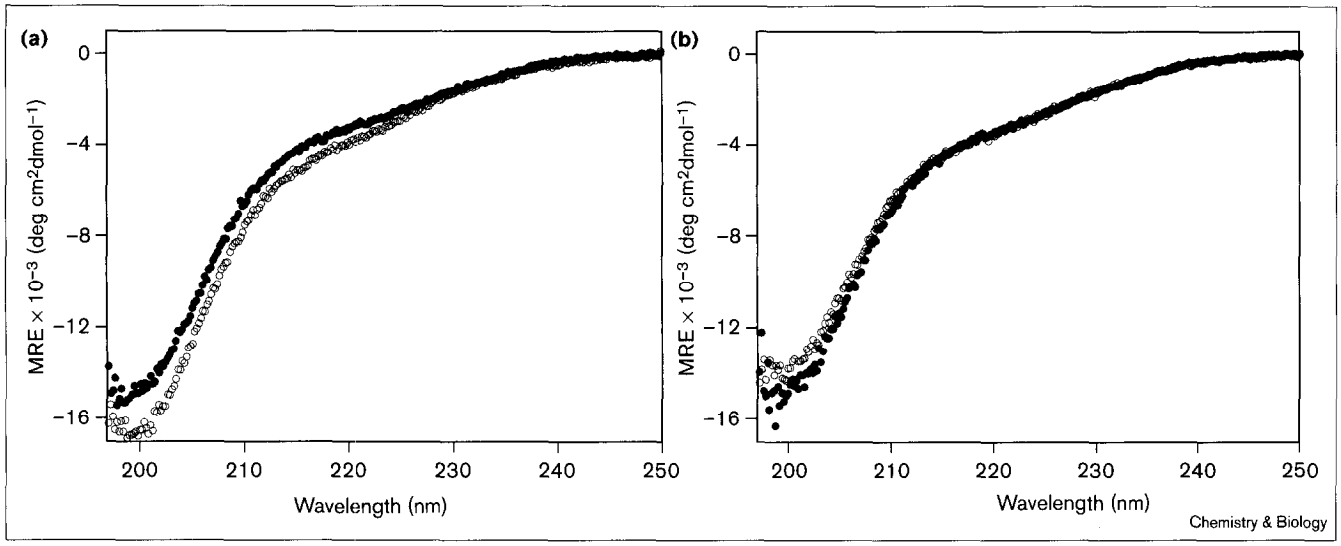

Far-UV CD evaluation of gelsolin GS–173–243 secondary structure as a function of pH. **(a)** Spectra of a 25 μM solution of wild-type gelsolin GS–173–243 at pH 4.0 (○; 50 mM sodium acetate) and at pH 7.0 (●; 50 mM sodium phosphate), both with100 mM NaCl at 4°C. **(b)** Spectra of D187N GS–173–243 gelsolin at pH 4.0 (○) and at pH 7.0 (●) under the same conditions as used in (a).

that has substantial circumstantial support, but has yet to be proven. Inhibiting amyloid fibril formation with small molecules is one approach to critically test the amyloid hypothesis in humans [55,56]. To develop inhibitors it is important to understand the process of amyloid fibril formation in some detail and in particular to identify the rate determining step(s). In the case of amyloidogenic proteins that have well-defined tertiary structures (e.g. transthyretin, lysozyme and the immunoglobulin light chains) a significant tertiary structural change occurs as a result of a mutation and/or a partially denaturing environment that allows the protein to adopt an alternative conformation (typically less structured), which self-assembles into amyloid fibrils. These mutations can affect both the kinetics and thermodynamics of the partial denaturation process, making the formation of the amyloidogenic conformational intermediate occur faster and to a greater extent [35–38,57].

The data presented within demonstrate that the gelsolin GS–173–243 fragment is a largely unstructured peptide that probably undergoes fibril formation via a different mechanism than that exhibited by folded proteins, at least in the initial stages [9]. The self-assembly of GS–173–243 and the change in structure from an unordered conformation to a β-sheet conformation associated with gelsolin amyloid fibril formation appears to be thermodynamically linked. This type of association-driven increase in structure is also a characteristic of the conversion of the Aβ peptide into the amyloid fibrils associated with Alzheimer's disease [52,58–63]. Amyloidogenic proteins therefore represent a structural continuum (structured to unstructured), yet both extremes of this continuum can form amyloid fibrils that are very similar in structure *in vivo* and *in vitro*, albeit by

Figure 8

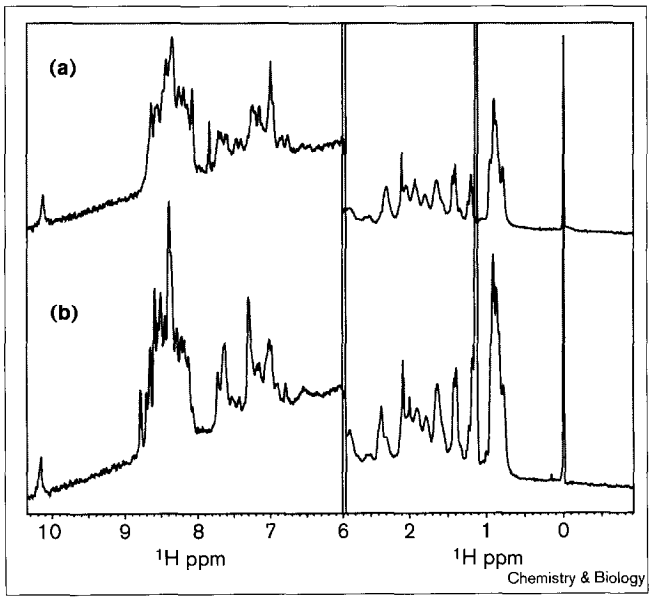

Utilizing one-dimensional ^{1}H NMR studies of D187N GS–173–243 gelsolin (100 μM) to evaluate the extent of defined structure. **(a)** The upfield aliphatic region and the downfield amide region of the ^{1}H NMR spectrum of D187N at pH 7.4 (10°C) is displayed. **(b)** The same regions of the ^{1}H NMR spectra of D187N gelsolin are displayed for the sample studied at pH 4.4.

Figure 9

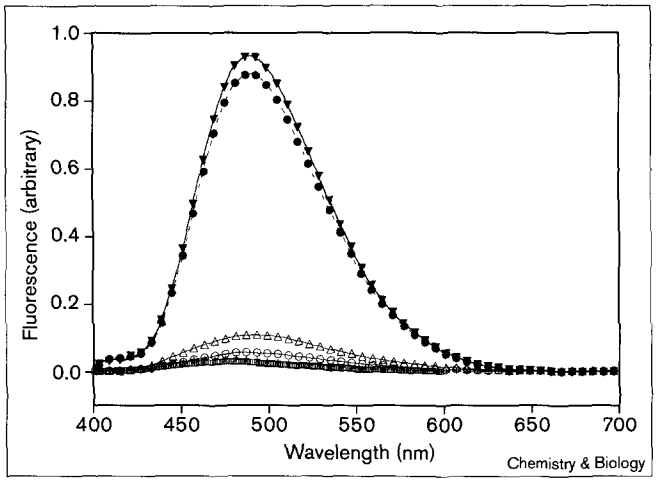

An analysis of the binding of ANS (50 μM) to wild-type and D187N gelsolin (5 μM) as a function of pH using fluorescence emission spectroscopy. The data collected at pH 7.4 (50 mM phosphate; □), pH 4.4 (50 mM acetate; △) and pH 2.0 (10 mM HCl, 100 mM NaCl; ▼) are shown. The same analysis for the D187N variant at pH 7.4 (+), pH 4.4 (○) and pH 2.0 (●) exhibits very similar results.

mechanisms that probably differ significantly in the early steps, but have common late steps [50,64]. The similarity of the final amyloid structures and the majority of the later intermediates suggest that the major difference between the assembly of initially unordered peptides and structurally defined proteins probably occurs at the very earliest steps of the amyloid fibril formation mechanism(s).

Gelsolin and Aβ amyloid fibril formation are similar in that the fibrils are composed of protein fragments produced from large parent proteins. Two proteolytic cuts in a large precursor protein appears to be the enabling event in Aβ fibril formation and is required, but not sufficient, for gelsolin amyloidosis [65–68]. Gelsolin fibril formation also appears to require an environmental change to convert the fragment into amyloid fibrils. It is interesting that amyloid formation is not observed for the full-length gelsolin protein. The most likely explanation for this is the high kinetic barriers that are associated with the conversion of a large folded protein into an intermediate that can self-assemble into amyloid fibrils. The activation free energy for converting peptides into amyloid fibrils is much lower, based on the numerous peptides that form amyloid-like deposits [13,14]. Not all peptides are capable of amyloid formation, however. There are at least two requirements for peptides to form amyloid fibrils: one or more components of the conformational ensemble exhibited by the peptide must be capable of adopting an assembly competent conformation; and the sequence has to be compatible with the higher-order assembly process associated with amyloid fibril formation. Ongoing studies of the D187N gelsolin amyloid-assembly mechanism might clarify the latter requirements. Because gelsolin is exclusively monomeric and nonamyloidogenic at pH 7.5, it is likely that pH triggering will facilitate an excellent understanding of the early stages of the mechanism of amyloid fibril formation.

Significance

Gelsolin is an actin-binding and modifying protein that undergoes two endo proteolytic cuts to afford the 71-residue amyloidogenic fragment. The main purpose of this work was to characterize the conformational properties and amylodogenicity of this fragment. This study demonstrates that it is possible to overexpress and purify the GS–173–243 gelsolin fragment that incorporates the sequence found in the amyloid fibrils of Finnish type familial amyloidosis (FAF) patients [5]. Biophysical studies demonstrate that both the wild-type and D187N FAF-associated fragments are largely unstructured monomeric peptides that cannot spontaneously convert to fibrils, even after one month of incubation at pH 7.5 (37 C). Slightly acidic conditions rapidly transform the wild-type and D187N amyloidogenic fragment into well defined fibrils, however. These results imply that proteolysis is necessary, but not sufficient, for gelsolin fibril formation. A low pH or analogous environmental change is also required for gelsolin GS–173–243 amyloid fibril formation *in vitro* on an experimental time scale. The inability of wild-type gelsolin to be amyloidogenic in humans appears to result from the resistance of the six-domain protein to proteolysis. In contrast, the D187N mutation appears to destabilize domain 2, making it susceptible to proteolysis, which affords the 71-residue internal amyloidogenic fragment that self-assembles into amyloid fibrils, possibly in an acidic organelle *in vivo*. Ongoing biophysical studies will critically evaluate the expected influence of the D187N mutation on gelsolin domain 2 stability. Hydrodynamic and microscopy studies on the assembly of the gelsolin D187N amyloidogenic fragment could provide further insight into the early stages of the amyloid fibril-formation mechanism.

Materials and methods

Cloning and expression of wild-type GS–173–243 gelsolin

The cDNA sequence of human plasma gelsolin, coding for amino acids Ala173–Met 243, which is amyloidogenic upon the introduction of a point mutation at position 187, was synthesized using the polymerase chain reaction (PCR) using full-length plasma gelsolin cDNA template (GenBank accession number X04412) and oligodeoxyribonucleotide primers 1 and 2. Sense strand primer 1 (5′-ACT GGA TCC GCC ACC GAG GTA CCT GTG TCC-3′) with a *Bam*HI restriction site and antisense primer 2 (5′-ATC AAG CTT TCA CAT CGC CTC GGG CTC AGT-3′) with a *Hind*III site were used to amplify the target cDNA using proof-reading Deep Vent DNA polymerase (New England Biolabs) according to the manufacturer's recommendations. The thermocycling reaction was performed in a MJ Research Minicycler (Watertown, MA) after an initial 5 min denaturation period at 94°C using the following cycle profile: 94°C for 30 s, 55°C for 30 s and 72°C for 30 s. Following a total of 25 cycles, a final extension period at 72°C was added for 10 min.

The wild-type gelsolin fragment generated in the PCR reaction was cloned into the *Bam*HI and *Hind*III sites of a modified glutathione S-transferase (GST) fusion vector, pGAT2, and expressed in *E. coli* BL21 (DE3) Epicurian Gold cells (Stratagene) in the form of a amino-terminal His-tagged, GST-fusion protein [15]. Protein production was carried out at 37°C in LB media supplemented with 100 μg/ml ampicillin following induction with 1 mM isopropyl-β-D-thiogalactopyranoside (IPTG). After 5–6 h of growth, the cells were concentrated by centrifugation, resuspended in phosphate buffered saline (PBS), and stored at −80°C until needed.

Purification of the fusion protein was achieved by passing the total cell lysate through Glutathione Sepharose 4B affinity resin (Pharmacia) as recommended by the manufacturer, followed by elution with a solution of 10 mM reduced glutathione (Calbiochem) dissolved in 50 mM Tris–HCl, pH 8.0. Direct addition of bovine thrombin (Sigma T4648) to the eluant from the glutathione column at a ratio of 0.2 units of enzyme per milligram of fusion protein liberated the gelsolin peptide that had two additional amino-terminal residues, glycine (−2) and serine (−1) from the His-tagged, GST-fusion protein. Following 4 h of proteolysis at room temperature with gentle mixing on a lab rotator, cleaved GST was removed from the target peptide by passing the reaction mixture through Ni-NTA-Agarose resin (Qiagen). The eluant from the Ni-NTA column, which contained the gelsolin fragment, was concentrated by ultrafiltration with a YM3 membrane (Amicon) and then purified to homogeneity by gel permeation chromatography on a HiLoad 26/60 Superdex 30 column (Pharmacia). An SDS–PAGE gel modified for peptides and small proteins was used to visualize the gelsolin fragment to confirm its presence and purity [69]. The identity of the purified gelsolin fragment was confirmed by cDNA sequencing and by electrospray mass spectrometry.

D187N and D187Y amyloidogenic mutants

The two point mutations that are found in the gelsolin amyloid deposits of FAF patients both occur at position 187, and involve replacing an aspartate residue with either a tyrosine or asparagine reside. These two mutations were synthesized using the QuickChange Site-Directed Mutagenesis protocol from Stratagene with wild-type gelsolin 173–243 fragment as the template. The D187Y mutant (nucleotide base change from G to T at position 654) was generated using the oligodeoxyribonucleotide 5′-GCT TCA ACA ATG GCT ACT GCT TCA TCC TGG-3′ and its inverse complement, whereas the oligodeoxyribonucleotide 5′-GCT TCA ACA ATG GCA ACT GCT TCA TCC TGG-3′ and its inverse complement were used to introduce the D187N mutation (nucleotide base change from G to A). Fourteen cycles each for 30 s at 95°C for denaturation, 1 min at 55°C for annealing and 12 min at 68°C for primer extension were executed to introduce the mutations at position 187. The presence of both mutations was confirmed by cDNA sequencing. Production and purification of the amyloidogenic gelsolin fragments was carried out as detailed above for the wild-type gelsolin peptide. The D187N peptide was used for the majority of our studies, although future work will also evaluate the GS 173–243 gelsolin D187Y variant using the studies described within. Preliminary results (pH independent fluorescence anisotropy values and amyloid formation below pH 6.0 only) suggest that D187Y mutant behaves similar to the D187N mutant studied here.

Gelsolin fibril formation assays

Sample preparation. Solutions of the purified gelsolin fragments (173–243) at both 2.5 and 25 μM were prepared from a stock solution of gelsolin (0.1 mM in PBS pH 7.4) by dilution into either 50 mM phosphate (pH 7.4 to 6.0) or 50 mM acetate (pH 6.0–4.0) buffer solutions containing 100 mM NaCl. The dilution buffers differed from one another by 0.5 pH units, allowing the amyloidogenicity to be evaluated over the pH range from 4–7.5. These samples were incubated without any agitation at 37°C or 4°C for 3–5 days before the light scattering and Congo red binding assays were performed. All samples were assayed in triplicate. Some samples from the above assays were further incubated at 37°C and evaluated after 2 months of stagnant incubation to discern if fibril formation was occuring, albeit slowly. Grid searches by electron microscopy were conducted for representative samples to further scrutinize amyloid fibril formation.

Light scattering assay. The stationary samples were vortexed for a few seconds to distribute the fibrils evenly. The sample (400 μl) was transferred to a quartz cuvette and the optical density at 330 nm was recorded on a Hewlett Packard 8543 UV/Vis spectrophotometer. The three values obtained at each pH were averaged and plotted using Kaleidograph.

Congo Red binding assay. A procedure developed by Klunk *et al.* [16] was used to ensure that the light scattering detected came from amyloid as opposed to amorphous aggregates. Vortexed samples of the gelsolin fragments (100 μl) were added to 550 μl of a 10 μM solution of freshly prepared Congo red that was purified by recrystallization. The solutions were incubated at room temperature for 1 h before the absorbance spectra were recorded. The amount of Congo red bound to the fibrils was determined by the following relationship:

$$\text{moles of CR bound/l of amyloid suspension} = (A_{540}/25295) - (A_{477}/46306)$$

The three values obtained at each pH were averaged and plotted using Kaleidograph.

FT–IR spectroscopy of the fibrils

Fibrils were obtained by incubating 25 μM solutions of the wild-type or D187N GS–173–243 gelsolin fragments at pH 4.0 (50 mM acetate, 100 mM NaCl in 100% D_2O) at 37°C for 2 weeks. The pH was uncorrected for isotope effects. Soluble protein not converted to fibrils was removed by centrifuging the suspensions at 14,000 rpm using a table-top microfuge and discarding the supernatant. The fibrils were washed a second time by resuspending the fibrils in buffer, centrifuging and discarding the supernatant. The fibrils were then applied to CaF_2 plates and dried under vacuum in a dessicator. Infrared spectra from 1000 cm^{-1} to 4000 cm^{-1} were recorded on a Nicolet Magna FT–IR spectrometer equipped with an MCT detector at room temperature. The resolution was 4 cm^{-1} and 512 scans were averaged for each sample. The spectra were then subtracted from that of the blank, which was acquired using a similar procedure using a CaF_2 plate without any sample applied. The data was smoothed and the band locations determined with the use of the second derivative spectra.

Evaluation of the gelsolin oxidation state by reverse-phase HPLC analysis

Three samples each of wild-type and D187N gelsolin (100 μl of a 50 μM solution), were prepared for this analysis. The first set of gelsolin GS-(173–243) samples (wild-type and D187N) was derived from an aliquot of freshly purified gelsolin polypeptide obtained immediately after the gel filtration chromatography, as described in the purification protocol. The second set of samples was prepared by treating wild-type and D187N gelsolin 173–243 with 30 mM DTT at room temperature for 30 min to ensure complete reduction of the disulfide bond. The third set of gelsolin samples (wild-type and D187N 173–243) was treated with an oxidative reshuffling buffer (3 mM cystine, 0.3 mM cysteine, 1 mM EDTA at pH 9.0) to ensure complete oxidation [70,71]. The HPLC chromatograms for a C_{18} reverse phase (Vydac C18 analytical) analysis for all of these samples were obtained using a 5 to 80% linear gradient of solvent B over 45 min (solvent A: 95% water, 5% acetonitrile, 0.1% TFA and solvent B: 95% acetonitrile, 5% water, 0.1% TFA). The reduced peptides eluted from the column with a retention time of 25 min (46% B) whereas the oxidized disulfide-linked peptides eluted with a retention time of 22 min (41% B).

Electron microscopy

A fibril suspension (5 μl) derived from the samples used for the fibril-forming assays were applied to glow-discharged, carbon-coated copper grids (mesh size 200 Å) for 2 min and blotted with Whatman

filter paper to remove excess solution. The grids were then stained with a 1% uranyl acetate solution for 2 min and excess stain was blotted away with filter paper. The grids were air dried and examined with a Philips CM100 transmission electron microscope at 80 KeV.

Fluoresence anisotropy measurements

Single point polarization data were obtained for both wild-type and D187N GS–173–243 fragments of gelsolin as a function of pH (7.4 to 2.0). The initial sample was a 10 μM solution of gelsolin in PBS at pH 7.4. The pH of the sample was lowered throughout the course of the experiment by titrating the sample with aliquots of a dilute acetic acid solution until the required pH was obtained. Six data points were acquired for the D187N polypeptide and seven data points were acquired for the wild-type gelsolin fragment. In order to acquire data at pH 2.0, the sample was further titrated with dilute HCl. The experiments were performed at room temperature using a SLM-AMINCO 8100 Series 2 spectrofluorometer in a T-optic configuration to obtain simultaneous measurements of the vertical (⊥) and horizontal (||) emission components of the polarized light. The exitation wavelength was 280 nm and the emission wavelength was 350 nm. Twenty five scans were averaged at each pH value with an integration time of 3 s, which was sufficient to obtain a standard deviation of 0.001 anisotropy units or less. The averaged data was plotted using Kaleidograph.

The fluorescence emission anistropy is defined as $(A) = I_{||} - I_{\perp} / I_{||} + 2I_{\perp}$ [72]; where $I_{||}$ is the emission intensity parallel to the plane of excitation and $I_{\perp}$ is the emission intensity perpendicular to the plane of excitation.

NMR spectroscopy

Wild-type and D187N gelsolin (GS–173–243) samples (0.1 mM) in PBS buffer at pH 7.4. (90% H_20, 10% D_20) were prepared. The ^1H one-dimensional NMR spectrum was recorded with a spectral width of 8064 Hz at pH 7.4 and 4.4. The pH of the PBS buffered sample was lowered by adding deuterated acetic acid until the desired pH of 4.4 was reached to record the data at lower pH. All spectra were acquired on a Bruker AMX500 spectrometer operating at 499.87 MHz at a probe temperature of 10°C. Water suppression was achieved employing the water gate sequence and 512 scans were averaged for each sample. An exponential window function was applied to the interferograms before fourier transformation. The data was processed using NMRPipe and NMRDraw (NIH software) on a Silicon Graphics Indigo 2 workstation. The spectra were referenced to TSP (0.0 ppm) which was added to the sample.

H-D exchange NMR experiments

Protein samples were dialysed into water and lyophilized. The GS–173–243 gelsolin fragment (0.4 mgs) was added to 400 μl of PBS buffer at pH 7.4 (100% D_20, pH uncorrected for D isotope effects), yielding a final protein concentration of 0.1 mM. The one-dimensional ^1H spectra of these samples were acquired within 5 min of dissolution. For each sample 32 scans were collected, with a spectral width of 8064 Hz. The data were processed as described above.

8-Anilino-1-naphthalenesulfonic acid (ANS) binding

A stock solution of 8-anilino-1-naphthalene sulfonic acid (ANS; Sigma A5144) prepared in deionized H_20 was added to both the wild-type and D187N (GS–173–243) gelsolin peptides producing samples with a final ANS concentration of 50 μM and a peptide concentration of 5 μM. The ANS concentration was determined by UV absorbance measurements at 372 nm using a molar extinction coefficient of 7800 M^{-1} cm^{-1}. Wild-type and D187N (GS–173–243) gelsolin peptides at pH 7.4 and pH 4.4 were prepared by dialysis against 50 mM sodium phosphate, pH 7.4 and 50 mM sodium acetate, pH 4.4, respectively. Preparations of gelsolin samples at pH 2.0 were made from lyophilized gelsolin which was initially resuspended in a solution of 10 mM HCl and 100 mM NaCl and then adjusted to the desired pH. The final volume of each sample analyzed was 1.0 ml. Fluorescence emission spectra were recorded on an Aviv Model ATF105 automated titrating differential/ratio spectrofluorometer at 25°C using an excitation wavelength of 375 nm with both the excitation and emission slit widths set to 2 mm.

Far-UV CD studies

All CD studies were performed on an AVIV Model 202SF Stopped Flow Circular Dichroism Spectrometer (Lakewood, NJ) equipped with a Peltier temperature-controlled cell holder. The CD spectra represented in Figure 7 are averages of three consecutive steady state scans which were corrected by subtracting a buffer blank (time constant of 100 msec, sampling at 0.2 nm intervals). Far-UV CD spectra were collected on 25 μM solutions of wild-type and D187N GS–173–243 peptides in 50 mM sodium phosphate (pH 7.4) or 50 mM sodium acetate buffer (pH 4.0), 100 mM NaCl at 4°C in a 0.1 cm pathlength quartz cell and are reported in units of mean residue ellipticity (MRE).

Supplementary material

Supplementary material demonstrating that the wild-type and D187N gelsolin fragments are monomeric (25 μM) at pH 7.4 (and therefore suitable for amyloidogenicity and biophysical studies) is available with the online version of this paper.

Acknowledgements

We thank the Lita Annenberg Hazen Family, the Skaggs Family, and the Baxter Family for infrastructure support, Dave Millar and Liz Thompson for help with the fluorescence anisotropy measurements, Les Burtnick for the gelsolin coordinates, as well as Hilal Laushel for his ultracentrifuge expertise. This work was primarily supported by the National Institutes of Health Grant R01 DK46335.

References

1. Kwiatkowski, D.J., Stossel, T.P., Orkin, S.H., Mole, J.E., Colten, H.R. & Yin, H.L. (1986). Plasma and cytoplasmic gelsolins are encoded by a single gene and contain a duplicated actin-binding domain. *Nature* **323**, 455-458.
2. Yin, H.L. (1987). Gelsolin: calcium- and polyphosphoinositide-regulated actin-modulating protein. *BioEssays* **7**, 176-179.
3. Janmey, P.A., Stossel, T.P. & Allen, P.G. (1998). Deconstructing gelsolin: identifying sites that mimic or alter binding to actin and phosphoinositides. *Chem. Biol.* **5**, R81-R85.
4. Lee, W.M. & Galbraith, R.M. (1992). The extracellular actin scavenger system and actin toxicity. *N. Engl. J. Med.* **326**, 1335-1341.
5. Kiurus, S. (1998). Gelsolin-related familial amyloidosis, finish type (FAF), and its variants found worldwide. *Amyloid: Int. J. Exp. Clin. Invest.* **5**, 55-66.
6. Lansbury, P.T. (1992). In pursuit of the molecular structure of the amyloid plaque: new technology provides unexpected and critical information. *Biochemistry* **31**, 6865-6870.
7. Blake, C. & Serpell, L. (1996). Synchrotron X-ray studies suggest that the core of the transthyretin amyloid fibril is a continuous β-sheet helix. *Structure* **4**, 989-998.
8. Serpell, L.C., *et al.*, & Blake, C.C.F. (1995). Examination of the structure of the transthyretin amyloid fibril by image reconstruction from electron micrographs. *J. Mol. Biol.* **254**, 113-118.
9. Kelly, J.W. (1996). Alternative conformations of amyloidogenic proteins govern their behavior. *Curr. Opin. Struct. Biol.* **6**, 11-17.
10. Burtnick, L.D., Koepf, E.K., Grimes, J., Jones, E.Y., Stuart, D.I., Mclaughlin, P.J. & Robinson, R.C. (1997). The crystal structure of plasma gelsolin: implications for actin severing, capping, and nucleation. *Cell* **90**, 661-670.
11. Paunio, T., *et al.*, & Peltonen, L. (1998). Cells of the neuronal lineage play a major role in the generation of amyloid precursor fragments in gelsolin-related amyloidosis. *J. Biol. Chem.* **273**, 16319-16324.
12. Maury, C.P.J., Nurmiaho-Lassila, E.-L. & Rossi, H. (1994). Amyloid fibril formation in gelsolin-derived amyloidosis: definition of the amyloidogenic region and evidence of accelerated amyloid formation of mutant Asn187 and Tyr187 Gelsolin Peptides. *Lab. Invest.* **70**, 558-564.
13. Choo, D.W., Schneider, J.P., Graciani, N.R. & Kelly, J.W. (1996). Nucleated antiparallel β-sheet that folds and undergoes self-assembly: a template promoted folding strategy toward controlled molecular architectures. *Macromolecules* **29**, 355-366.
14. Yamada, N., Ariga, K., Naito, M., Matsubara, K. & Koyama, E. (1998). Regulation of β-sheet structures within amyloid-like β-sheet assemblage from tripeptide derivatives. *J. Am. Chem. Soc.* **120**, 12192-12199.
15. Macias, M.J., *et al.*, & Oschkinat, H. (1996). Structure of the WW domain of a kinase-associated protein complexed with a proline-rich peptide. *Nature* **382**, 646-649.

16. Klunk, W.E., Pettegrew, J.W. & Abraham, D.J. (1989). Quanitative evaluation of congo red binding to amyloid-like proteins with a β-pleated sheet conformation. *J. Histochem. Cytochem.* **37**, 1273-1281.
17. Fraser, P.E., Nguyen, J.T., Inouye, H., Surewicz, W.K., Selkoe, D.J., Podlisny, M.B. & Kirschner, D.A. (1992). Fibril formation by primate, rodent, and Dutch-hemorrhagic analogues of Alzheimer amyloid β-protein. *Biochemistry* **31**, 107160-10723.
18. Valuer, B. & Weber, G. (1977). Resolution of the fluorescence excitation spectrum of indole into the 1La and 1Lb excitation bands. *Photochem. Photobiol.* **25**, 441-444.
19. Wüthrich, K. (1986). *NMR of Proteins and Nucleic Acids.* Wiley Interscience, New York.
20. Goto, Y., Takahashi, N. & Fink, A.L. (1990). Mechanism of acid induced folding of proteins. *Biochemistry* **29**, 3480-3488.
21. Goto, Y., Calciano, L.J. & Fink, A.L. (1990). Acid-induced folding of proteins. *Proc. Natl Acad. Sci. USA* **87**, 573-577.
22. Fink, A.L., Calciano, L.J., Goto, Y., Kurotsu, T. & Palleros, D. (1994). Classification of acid denaturation of proteins: intermediates and unfolded states. *Biochemistry* **41**, 12504-12511.
23. Goto, Y. & Fink, A.L. (1989). Conformational studies of b-lactamase: Molten globule states at acidic and alkaline pH with high salt. *Biochemistry* **28**, 945-952.
24. Ghiso, J., Haltia, M., Prelli, F., Novello, J. & Frangione, B. (1990). Gelsolin variant (Asn187) in familial amyloidosis, Finnish type. *Biochem. J.* **272**, 827-830.
25. Levy, E., *et al.*, & Frangione, B. (1990). Mutation in gelsolin gene in Finnish hereditary amyloidosis. *J. Exp. Med.* **172**, 1865-1868.
26. Haltia, M., *et al.*, & Frangione, B. (1990). Amyloid protein in familial amyloidosis (Finnish type) is homologous to gelsolin, an actin-binding protein. *Biochem. Biophys. Res. Commun.* **167**, 927-932.
27. Maury, C.P.J., Kere, J., Tolvanen, R. & De la Chapelle, A. (1990). Finnish hereditary amyloidosis is caused by a single nucleotide substitution in the gelsolin gene. *FEBS Lett.* **276**, 75-77.
28. Maury, C.P.J., Alli, K. & Baumann, M. (1990). Finnish hereditary amyloidosis. Amino acid sequence homology between the amyloid fibril protein and human plasma gelsolin. *FEBS Lett.* **260**, 85-87.
29. Paunio, T., Kangas, H., Kalkkinen, N., Haltia, M., Palo, J. & Peltonen, L. (1994). Toward understanding the pathogenic mechanisms in gelsolin-related amyloidosis: *in vitro* expression reveals an abnormal gelsolin fragment. *Hum. Mol. Genet.* **3**, 2223-2239.
30. Kangas, H., Paunio, T., Kalkkinen, N., Jalanko, A. & Peltonen, L. (1996). *In vitro* expression analysis shows that the secretory form of gelsolin is the sole source of amyloid in gelsolin-related amyloidosis. *Hum. Mol. Genet.* **5**, 1237-1243.
31. Maury, C.P.J., Sletten, K., Totty, N., Kangas, H. & Liljestrom, M. (1997). Identification of the circulating amyloid precursor and other gelsolin metabolites in patients with G654A mutation in the gelsolin gene (Finnish familial amyloidosis): pathogenetic and diagnostic implications. *Lab. Invest.* **77**, 299-304.
32. Paunio, T., Kiuru, S., Karonen, S.-L., Palo, J. & Peltonen, L. (1994). Quantification of serum and cerebrospinal fluid gelsolin in familial amyloidosis, Finnish type (AGel). *Amyloid* **1**, 80-89.
33. Maury, C.P.J. & Rossi, H. (1993). Demonstration of a circulating 65K gelsolin variant specific for familial amyloidosis, Finnish type. *Biochem. Biophys. Res. Commun.* **191**, 41-44.
34. Sunada, Y., Sakurai, T., Nonomura, Y. & Kanazawa, I. (1994). Abnormal gelsolin fragments in the patients with familial amyloidosis of the Finnish type. In *Amyloid Amyloidosis 1993: The Proceedings of the VII International Symposium on Amyloidosis, July 11-15, Kingston, Ontario, Canada.* (Kisilevsky, R., Benson, M.D., Frangione, D., Gauldie, J., Muckle, T.J., & Young, I.D., eds.) pp 623-625, Parthenon Publications, New York.
35. Colon, W. & Kelly, J.W. (1992). Partial denaturation of transthyretin is sufficient for amyloid fibril formation *in vitro*. *Biochemistry* **31**, 8654-8660.
36. Lai, Z., Colon, W. & Kelly, J.W. (1996). The acid-mediated denaturation pathway of transthyretin yields a conformational intermediate which can self-assemble into amyloid. *Biochemistry* **35**, 6470-6482.
37. McCutchen, S., Colon, W. & Kelly, J.W. (1993). Transthyretin mutation Leu55→Pro significantly alters tetramer stability and increases amyloidogenicity. *Biochemistry* **32**, 12119-12127.
38. McCutchen, S. L., Lai, Z., Miroy, G., Kelly, J.W. & Colon, W. (1995). Comparison of lethal and non-lethal transthyretin variants and their relationship to amyloid disease. *Biochemistry* **34**, 13527-13536.
39. Chan, S.L., Chronopoulos, S., Murray, J., Laird, D.W. & Ali-Khan, Z. (1997). Selective localization of murine ApoSAA1/SAA2 in endosomes-lysosomes in activated macrophages and their degradation products. *Amyloid* **4**, 40-48.
40. Charge, S.B.P., de Koning, E.J.P. & Clark, A. (1995). Effect of pH and insulin on fibrillogenesis of islet amyloid polypeptide *in vitro*. *Biochemistry* **34**, 14588-14593.
41. Fraser, P.E., Nguyen, J.T., Surewicz, W.K. & Kirschner, D.A. (1991). pH-Dependent structural transitions of Alzheimer amyloid peptides. *Biophys. J.* **60**, 1190-1201.
42. Guijarro, J.I., Sunde, M., Jones, J.A., Campbell, I.D. & Dobson, C.M. (1998). Amyloid fibril formation by an SH3 domain. *Proc. Natl Acad. Sci. USA* **95**, 4224-4228.
43. Wood, S.J., Wetzel, R. & Hurle, M.R. (1994). In *Amyloid Amyloidosis 1993, The Proceedings of the VII International Symposium on Amyloidosis, July 11-15, Kingston, Ontario, Canada.* (Kisilevsky, R., Benson, M.D., Frangione, D., Gauldie, J., Muckle, T.J., & Young, I.D., eds.) pp 523-525, Parthenon Publications. New York.
44. Cataldo, A.M., Hamilton, D.J., Barnett, J.L., Paskevich, P.A. & Nixon, R.A. (1996). Properties of the endosomal-lysosomal system in the human central nervous system: disturbances mark most neurons in populations at risk to degenerate in Alzheimer's disease. *J. Neurosci.* **16**, 186-199.
45. Chan, S.L., Chronopoulos, S., Murray, J., Laird, D.W. & Ali-Khan, Z. (1997). Selective localization of murine ApoSAA1/SAA2 in endosomes-lysosomes in activated macrophages and their degradation products. *Amyloid* **4**, 40-48.
46. De Koning, E.J.P., *et al.*, & Clark, A. (1993). Localization of islet amyloid polypeptide (IAPP) in pancreatic islets of transgenic mice expressing the human or rat IAPP gene. *Biochem. Soc. Trans.* **21**, 26s.
47. Mayer, R.J., *et al.*, & Landon, M. (1996). Endosome-lysosomes, ubiquitin and neurodegeneration. *Adv. Exp. Med. Biol.* **389**, 261-269.
48. Shirahama, T. & Cohen, A.S. (1975). Intralysosomal formation of amyloid fibrils. *Am. J. Pathol.* **81**, 101-116.
49. Shirahama, T., Miura, K., Ju, S.-T., Kisilevsky, R., Gruys, E. & Cohen, A.S. (1990). Amyloid enhancing factor-loaded macrophages in amyloid fibril formation. *Lab. Inv.* **62**, 61-68.
50. Harper, J.D., Wong, S.S., Lieber, C.M. & Lansbury, P.T., Jr. (1997). Observation of metastable Ab amyloid protofibrils by atomic force microscopy. *Chem. Biol.* **4**, 119-125.
51. Lambert, M.P., *et al.*, & Krafft, G.A. (1998). Diffusable, nonfibrillar ligands derived from Ab1-42 are potent central nervous system toxins. *Proc. Natl Acad. Sci. USA* **95**, 6448-6453.
52. Jarrett, J. & Lansbury, P.T. (1993). Seeding one -dimensional crystallization of amyloid: a pathogenic mechanism in Alzheimer's disease and Scrapie? *Cell* **73**, 1055-1058.
53. Kelly, J.W. (1997). Amyloid fibril formation and protein misassembly: a structural quest for insights Into amyloid and prion diseases. *Structure* **5**, 595-600.
54. Kelly, J.W. (1998). The alternative conformations of amyloidogenic proteins and their multi-step assembly pathways. *Curr. Opin. Struct. Biol.* **8**, 101-106.
55. Miroy, G.J., Lai, Z., Lashuel, H., Peterson, S.A., Strang, C. & Kelly, J.W. (1996). Inhibiting transthyretin amyloid fibril formation via protein stabilization. *Proc. Natl Acad. Sci. USA* **93**, 15051-15056.
56. Peterson, S.A., Klabunde, T., Lashuel, H.A., Purkey, H., Sacchettini, J.C. & Kelly, J.W. (1998). Inhibiting transthyretin conformational changes that lead to amyloid fibril formation. *Proc. Natl Acad. Sci. USA* **95**, 12956-12960.
57. Lai, Z., McCulloch, J. & Kelly, J.W. (1997). GdnHCl-induced denaturation and refolding of transthyretin exhibits a marked hysteresis: equilibria with high kinetic barriers. *Biochemistry* **36**, 10230-10239.
58. Lee, S.-J., Liyanage, U., Bickel, P.E., Xia, W., Lansbury, P.T., Jr & Kosik, K.S. (1998). A detergent-insoluble membrane compartment contains A–β *in vivo*. *Nat. Med.* **4**, 730-734.
59. Lansbury, P.T., Jr. (1997). Inhibition of amyloid formation: a strategy to delay the onset of Alzheimer's disease. *Curr. Opin. Chem. Biol.* **1**, 260-267.
60. Lansbury, P.T., Jr. (1997). Structural neurology: are seeds at the root of neuronal degeneration? *Neuron* **19**, 1151-1154.
61. Lansbury, P.T., Jr. (1996). A reductionist view of Alzheimer's disease. *Accounts Chem. Res.* **29**, 317-321.
62. Come, J.H., Fraser, P.E. & Lansbury, P.T., Jr. (1993). A kinetic model for amyloid formation in the prion diseases: importance of seeding. *Proc. Natl Acad. Sci. USA* **90**, 5959-5963.
63. Harper, J.D. & Lansbury, P.T., Jr. (1997). Models of amyloid seeding in Alzheimer's disease and scrapie: mechanistic truths and physiological consequences of the time-dependent solubility of amyloid proteins. *Annu. Rev. Biochem.* **66**, 385-407.

64. Snyder, S.W., *et al.*, & Holzman, T.F. (1994). Amyloid-β aggregation: selective inhibition of aggregation in mixtures of amyloid with different chain lengths. *Biophys. J.* **67**, 1216-1228.
65. Golde, T.E., Estus, S., Younkin, L.H., Selkoe, D.J. & Younkin, S.G. (1992). Processing of the amyloid protein precursor to potentially amyloidogenic derivatives. *Science* **255**, 728-730.
66. Shoji, M., *et al.*, & Younkin, S.G. (1992). Production of the Alzheimer amyloid β-protein by normal proteolytic processing. *Science* **258**, 126-129.
67. Selkoe, D.J. (1997). Alzheimer's disease: genotypes, phenotype and treatments. *Science* **275**, 630-631.
68. Selkoe, D.J. (1994). Cell biology of the amyloid beta-protein precursor and the mechanism of Alzheimer's disease. *Annu. Rev. Cell. Biol.* **10**, 373-403.
69. Schagger, H. & Von Jagow, G. (1987). Tricine-sodium dodecyl sulfate-polyacrylamide gel electrophoresis for the separation of proteins in the range from 1 to 100 kDa. *Anal. Biochem.* **166**, 368-379.
70. Xie, Y., Lashuel, H., Miroy, G.J., Dikler, S. & Kelly, J.W. (1998). Recombinant human retinol-binding protein refolding, native disulfide formation and characterization. *Protein Exp. Purif.* **14**, 31-37.
71. Wetlaufer, D.B., Branca, P.A. & Chen, G.X. (1987). The oxidative folding of proteins by disulfide plus thiols does not correlate with redox potential. *Protein Eng.* **1**, 141-146.
72. Bigger, S.W., Craig, R.A., Ghiggino, K.P. & Schiers, J. (1993). Fluorescence anistropy measurements in undergraduate teaching. *J. Chem. Edu.* **70**, A234-A239.
73. Kraulis, P.J. (1991). MOLSCRIPT: a program to produce both detailed and schematic plots of protein structures. *J. Appl. Crystallogr.* **24**, 946-950.

Because *Chemistry & Biology* operates a 'Continuous Publication System' for Research Papers, this paper has been published via the internet before being printed. The paper can be accessed from http://biomednet.com/cbiology/cmb – for further information, see the explanation on the contents pages.